

Journal of Biomedical Optics

SPIEDigitalLibrary.org/jbo

Reduced speed of microvascular blood flow in hemodialysis patients versus healthy controls: a coherent hemodynamics spectroscopy study

Michele L. Pierro
Jana M. Kainerstorfer
Amanda Civiletto
Daniel E. Weiner
Angelo Sassaroli
Bertan Hallacoglu
Sergio Fantini

Reduced speed of microvascular blood flow in hemodialysis patients versus healthy controls: a coherent hemodynamics spectroscopy study

Michele L. Pierro,^{a,†} Jana M. Kainerstorfer,^{a,*†} Amanda Civiletto,^b Daniel E. Weiner,^b Angelo Sassaroli,^a Bertan Hallacoglu,^a and Sergio Fantini^a

^aTufts University, Department of Biomedical Engineering, 4 Colby Street, Medford, Massachusetts 02155

^bTufts Medical Center, 800 Washington Street, Boston, Massachusetts 02111

Abstract. We present a pilot clinical application of coherent hemodynamics spectroscopy (CHS), a technique to investigate cerebral hemodynamics at the microcirculatory level. CHS relies on frequency-resolved measurements of induced cerebral hemodynamic oscillations that are measured with near-infrared spectroscopy (NIRS) and analyzed with a hemodynamic model. We have used cyclic inflation (200 mmHg) and deflation of a pneumatic cuff placed around the subject's thigh at seven frequencies in the range of 0.03 to 0.17 Hz to generate CHS spectra and to obtain a set of physiological parameters that include the blood transit times in the cerebral microcirculation, the cutoff frequency for cerebral autoregulation, and blood volume ratios across the three different compartments. We have investigated five hemodialysis patients, during the hemodialysis procedure, and six healthy subjects. We have found that the blood transit time in the cerebral microcirculation is significantly longer in hemodialysis patients with respect to healthy subjects. No significant differences were observed between the two groups in terms of autoregulation efficiency and blood volume ratios. The demonstration of the applicability of CHS in a clinical setting and its sensitivity to the highly important cerebral microcirculation may open up new opportunities for NIRS applications in research and in medical diagnostics and monitoring. © 2014 Society of Photo-Optical Instrumentation Engineers (SPIE) [DOI: 10.1117/1.JBO.19.2.026005]

Keywords: near-infrared spectroscopy; photon migration; hemodynamic oscillations; cerebral microcirculation; cerebral autoregulation, hemodialysis.

Paper 130692R received Sep. 23, 2013; revised manuscript received Jan. 8, 2014; accepted for publication Jan. 10, 2014; published online Feb. 12, 2014.

1 Introduction

The study of cerebral hemodynamic oscillations, by using a number of different techniques, has led to a series of important results that opened new opportunities for the investigation of brain function, physiology, and pathological conditions. For example, the study of spontaneous low-frequency oscillations (LFOs) (≤ 0.1 Hz), which reflect a combination of systemic cardiovascular dynamics and local metabolic and flow regulation effects,¹ has led to the assessment of resting state functional connectivity using functional magnetic resonance imaging² and near-infrared spectroscopy (NIRS).³ Different brain states, such as rest versus functional activation^{4,5} or different sleep stages,⁶ are also associated with different features of cerebral LFOs as measured with NIRS. Spontaneous cerebral blood flow oscillations (measured with transcranial Doppler ultrasound) and systemic arterial blood pressure oscillations (measured with finger plethysmography) have been used to assess cerebral autoregulation.⁷ Phase shifts measurements between hemodynamic and blood pressure oscillations typically require high coherence levels, for example >0.4 ⁷ or >0.5 ,⁴ and it was observed that cerebral hemodynamic oscillations induced by paced breathing feature a significantly higher coherence with respect to spontaneous LFOs.⁸ Because of their stronger coherence and reliability, induced hemodynamic oscillations have been elicited

by paced breathing,^{8,9} repeated head-up tilting,¹⁰ squat-stand maneuvers,¹¹ and cyclic thigh cuff inflation-deflation¹² at frequencies ~ 0.1 Hz. These approaches were typically aimed at eliciting quantifiable changes in cerebral autoregulation since the cyclic perturbations associated with paced breathing, head-up tilting, squat-stand maneuvers, and thigh cuff inflation-deflation all induce oscillations in the arterial blood pressure, so that measurements of the associated cerebral blood flow oscillations provide an assessment of cerebral autoregulation mechanisms. The vast majority of the studies in the literature were based on inducing oscillations at a single frequency, with a few exceptions in which multiple frequencies of paced breathing were considered, namely (0.10, 0.17, 0.25 Hz),⁹ (0.10, 0.25 Hz),¹³ and (0.10, 0.12, 0.17, 0.25, 0.50 Hz).¹⁴ These studies at multiple frequencies were aimed at assessing the effect of end-tidal CO₂, which is reduced at higher breathing rates,⁹ determining the optimal paced breathing frequency for baroreflex sensitivity assessment,¹³ and measuring the level of cross-correlation between the oscillations in the heart rate and blood pressure at different respiratory rates.¹⁴ Recently, we proposed a new kind of frequency-resolved measurement of induced cerebral hemodynamic oscillations, which we named coherent hemodynamics spectroscopy (CHS).¹⁵ CHS involves amplitude and phase measurements of the oscillations in the tissue concentrations of deoxy-hemoglobin (*D*), oxy-hemoglobin (*O*), and total hemoglobin (*T*) that are induced by periodic physiological

*Address all correspondence to: Jana M. Kainerstorfer, E-mail: jana.kainerstorfer@tufts.edu

[†]These authors contributed equally to the work.

challenges at multiple frequencies. NIRS is an ideal technique for the measurement of D , O , and T , and in our first demonstration of CHS we have used paced breathing at 11 different frequencies (0.071, 0.077, 0.083, 0.091, 0.100, 0.111, 0.125, 0.143, 0.167, 0.200, 0.250 Hz) to obtain the CHS spectra that are based on the amplitude and phase of the oscillations of D , O , and T as a function of frequency.^{16,17} The high coherence between the driving oscillations in the arterial blood pressure and the induced, measured oscillations in the concentrations of oxy-, deoxy-, and total hemoglobin were exploited to model the cerebral microvasculature response as a linear time invariant system,¹⁵ providing a quantitative framework for CHS and allowing for the determination of a number of physiological parameters by fitting the measured CHS spectra with the model equations.¹⁸ It is the combination of (A) the richer information content of frequency-resolved measurements of hemodynamic oscillations, and (B) the quantitative framework provided by the new hemodynamic model¹⁵ that accounts for the innovation of CHS and for its ability to yield specific physiological parameters related to the cerebral microcirculation. Specifically, measurable physiological parameters with CHS include the speed of blood flow in the cerebral microvasculature, the distribution of blood volume and its dynamic changes in the arterial, capillary, and venous compartments, and autoregulation effectiveness at the microvascular level.

In this work, we further develop the CHS technique by demonstrating its applicability in a clinical setting, namely the hemodialysis unit. We collected CHS spectra by inducing coherent cerebral hemodynamic oscillations by means of cyclic thigh cuff inflation/deflation at multiple frequencies within the range of 0.03 to 0.17 Hz. Hemodialysis patients are an ideal population to evaluate the clinical applicability of CHS, given the high prevalence of micro- and macrovascular disease, including cerebrovascular disease, a within-person changing hemodynamic environment over a short period of time that occurs as part of usual care, and possibly variable capacity for vascular autoregulation, all making for a vulnerable brain. Cardiovascular disease is the leading cause of death among dialysis patients, with 10- to 50-fold higher rates of cardiovascular mortality at any given age than in the general population.¹⁹ Although this increase in mortality may represent a more rapid development and progression of vascular disease in dialysis patients, it is also a manifestation of the increased incidence and prevalence of cardiovascular disease among people with kidney disease not yet on dialysis.²⁰ In late-stage kidney disease, much of the cardiovascular disease burden appears to affect the microvasculature, including the cerebrovascular circulation, and at all stages of kidney disease, but most notably in dialysis patients, there is a high risk of both clinically recognized stroke and subclinical cerebrovascular disease.^{21,22} Previous NIRS studies in the hemodialysis unit have found a lower baseline cerebral tissue oxygenation in hemodialysis patients compared to healthy controls²³ and peritoneal dialysis patients,²⁴ and a greater hemoglobin concentration and reduced microvascular compliance measured in the calf muscle as a result of hemodialysis.²⁵ The effect of hemodialysis on the regional cerebral blood flow has been investigated with Xenon ventilation scintigraphy, where a mild reduction in cerebral blood flow was shown following as compared to before hemodialysis,²⁶ and with magnetic resonance imaging, where dialysis patients had lower cerebral blood flow than healthy controls.²³ The effect on large artery blood flow velocity has been assessed with transcranial Doppler ultrasound, revealing a significant decrease in

blood flow velocity following dialysis as compared to prior to hemodialysis.^{27–33} Although some studies have reported a significantly lower regional cerebral blood flow in hemodialysis patients (before dialysis) versus healthy controls,³¹ other studies have not observed a significant difference in the regional cerebral blood flow²⁶ or in the middle cerebral artery flow velocity³² of hemodialysis patients (before dialysis) and healthy controls. There are limited dynamic studies conducted during the hemodialysis procedure.

Since the CHS is sensitive to the cerebral capillary and venous blood transit times, the vulnerable cerebral microvasculature in hemodialysis patients and the impact of hemodialysis on cerebral blood flow provide a valid benchmark to demonstrate the potential applicability of CHS to a clinical population, and to perform a comparison with a healthy control group. To induce hemodynamic oscillations at a given frequency, we have opted for cyclic thigh cuff inflation-deflation because it does not require any active involvement from the subject (as opposed to the paced breathing protocol), any movement (as opposed to squat-stand maneuvers or repeated head-up tilting), and it can be performed automatically in a highly reproducible fashion.

2 Methods

2.1 Data Acquisition and Measurement Protocol

The NIRS measurements were performed with a commercial frequency-domain tissue spectrometer (OxiplexTS, ISS, Inc., Champaign, Illinois) operating at a data acquisition rate of 6.25 Hz. The source–detector optode pair was held in place on the left side of the subject's forehead by a flexible headband. We avoided the central portion of the forehead because of the presence of the superior sagittal sinus, and either side of the forehead was suitable for this study aimed at global cerebrovascular effects. An additional black band was placed around the subject's head to exert a slight pressure on the optical probe to guarantee consistent skin contact and to prevent ambient light from reaching the detector. The source–detector separation was 3.5 cm. At the source location light was delivered at wavelengths of 690 and 830 nm. Detected light intensity changes at 690 and 830 nm were translated into oxy- and deoxy-hemoglobin concentrations in tissue (O and D) by utilizing the modified Beer–Lambert law³⁴ with a differential pathlength factor (DPF) obtained by using diffusion theory expressions in terms of the tissue optical properties.³⁵ We measured the tissue optical properties with multidistance frequency-domain spectroscopy,³⁵ resulting in DPF values in the range of 4.9 to 6.7 at 690 nm and 4.1 to 5.6 at 830 nm over all subjects examined.

To induce cerebral hemodynamic oscillations, a pneumatic cuff was placed around the left thigh of each participant and connected to an automated cuff inflation device (E-20 Rapid Cuff Inflation System, D. E. Hokanson, Inc., Bellevue, Washington). The thigh cuff was periodically inflated (to a pressure of ~200 mmHg) and deflated for four periods at seven different frequencies in the following order: 0.08, 0.17, 0.05, 0.10, 0.125, 0.07, and 0.03 Hz. A schematic diagram of the experimental setup is shown in Fig. 1. The effect of a cyclic inflation-deflation of the thigh cuff is to induce a cyclic increase–decrease of the arterial blood pressure.¹² The modulation of the arterial blood pressure determines oscillations in the cerebral

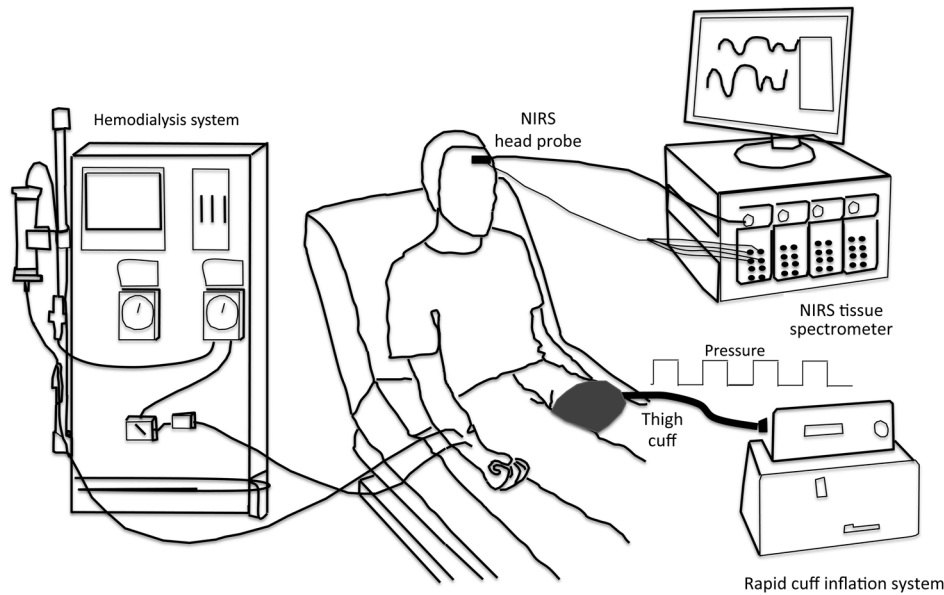


Fig. 1 Schematic diagram of the experimental setup for hemodialysis patients. Subjects were seated and a rapid cuff inflation system (E-20, D. E. Hokanson, Inc., Bellevue, Washington) was used to induce cerebral hemodynamic oscillations by cyclic inflation-deflation of a thigh cuff placed on the left thigh of the subject. Seven frequencies of oscillations were induced within the range 0.03 to 0.17 Hz. Near-infrared spectroscopy (NIRS) data were collected with an optical probe placed on the left side of the subjects' forehead (NIRS head probe). The optical probe was connected to a commercial tissue spectrometer (OxiplexTS, ISS, Inc., Champaign, Illinois). The experimental setup for healthy controls was the same as for hemodialysis patients, with the obvious difference of the absence of the hemodialysis system.

concentrations of deoxy-hemoglobin (D) and oxy-hemoglobin (O) that can be measured by NIRS.

The four periods of cyclic cuff inflation-deflation at a given frequency were followed by at least 1 min of rest to allow for subject recovery, with the rest time varying over all measured subjects from 1 to 10 min. These rest periods are not strictly required so that they may be avoided to reduce the measurement time for CHS spectra. All measurements on hemodialysis patients were performed within the first hour of dialysis treatment.

2.2 Human Subjects

Eleven subjects participated in the study: five patients undergoing hemodialysis treatment (HD, numbered 1 to 5) and six healthy adult volunteers (numbered 6 to 11). All participants gave their written informed consent prior to participating in this

study. Hemodialysis patients were recruited from a Boston area hemodialysis unit. The hemodialysis session was performed per the patient's usual treatment protocol via an upper extremity arteriovenous (AV) fistula or graft. Blood flow rates through the hemodialysis apparatus ranged from 300 to 450 ml/min. All dialysis sessions were clinically uneventful. Demographic and clinical characteristics for hemodialysis patients are reported in Table 1. Average age of the healthy subjects, 2 males and 4 females, was 27 y (range: 24 to 30 y). None of the healthy subjects had any record of cardiovascular or neurological disease.

2.3 Data Processing

For each frequency of induced oscillations (0.03 to 0.17 Hz), we performed Fourier analysis of the time traces of deoxy- and oxy-hemoglobin concentrations [$D(t)$ and $O(t)$]. We kept for

Table 1 Demographic and clinical characteristics of dialysis patients.

Subject ID	Gender	Age range	Dialysis duration	Previous smoker	Primary cause of ESRD	Peripheral vascular disease	Stroke	Diabetes	Myocardial infarction	MAP (mmHg)
1	F	60+	<1 year	No	Primary GN	No	No	No	No	85
2	F	20 to 40	5+ years	No	Secondary GN	No	No	No	No	82
3	F	60+	1 to 3 years	No	Diabetes	No	No	Yes	Yes	95
4	M	40 to 60	3 to 5 years	Yes	Diabetes	Yes	Yes	Yes	No	88
5	F	20 to 40	1 to 3 years	Yes	Secondary GN	Yes	No	No	No	92

Note: GN, glomerulonephritis; ESRD, end stage renal disease; MAP, mean arterial pressure.

further analysis only those trials for which the power spectra of both D and O showed a peak at the frequency of the cuff cyclic inflations. Temporal drifts were removed from all oxy- and deoxy-hemoglobin concentration signals by a third-order polynomial detrending. Detrended $D(t)$ and $O(t)$ temporal traces were then filtered by using a linear-phase band-pass finite impulse response filter based on the Parks–McClellan algorithm.³⁶ The center frequency of the band-pass filter (f_0) was set to the thigh cuff inflation/deflation frequency, and the filter’s bandwidth was set to $f_0 \pm 0.01$ Hz. Furthermore, we only considered those oscillations of D and O with an amplitude above a threshold value of $0.015 \mu\text{M}$ according to the noise level measured on tissue-like phantoms over the same bandwidth considered here.

Oscillations in the cerebral concentrations of deoxy- and oxy-hemoglobin were represented using phasor notation as $\mathbf{D}(\omega)$ and $\mathbf{O}(\omega)$,^{6,37} respectively, where ω is the angular frequency of the induced oscillations and the bold face indicate two-dimensional phasors defined in terms of the amplitude and phase of the oscillations. Based on this phasor representation, total hemoglobin phasors are given by a vector superposition of the phasors associated with the deoxy- and oxy-hemoglobin concentration oscillations: $\mathbf{T}(\omega) = \mathbf{D}(\omega) + \mathbf{O}(\omega)$. The amplitude and phase of the oscillations of deoxy- and oxy-hemoglobin concentrations [respectively $|\mathbf{D}|$ and $\text{Arg}(\mathbf{D})$, $|\mathbf{O}|$ and $\text{Arg}(\mathbf{O})$] were assessed by the analytic signal method^{6,38} as described previously.^{6,16,37}

2.4 Coherent Hemodynamics Spectroscopy (CHS)

The Coherent Hemodynamics Spectroscopy (CHS), recently proposed by Fantini,¹⁵ is based on frequency-resolved measurements of the amplitude and phase of the hemoglobin concentration phasors $\mathbf{D}(\omega)$, $\mathbf{O}(\omega)$, and $\mathbf{T}(\omega)$. In order to minimize the sensitivity to the frequency dependence of the amplitude of the oscillatory stimulation, the method is based on measuring amplitude ratios ($|\mathbf{D}|/|\mathbf{O}|$, $|\mathbf{O}|/|\mathbf{T}|$) and phase differences [$\text{Arg}(\mathbf{D})-\text{Arg}(\mathbf{O})$, $\text{Arg}(\mathbf{O})-\text{Arg}(\mathbf{T})$] of the induced hemodynamic oscillations.¹⁸ To average the phase values and amplitude ratios within a given stimulus frequency, we selected those time windows featuring oscillations with a stable phase, as assessed by a lack of monotonic change and/or phase slips³⁹ in the time dependence of the instantaneous phase differences $\text{Arg}(\mathbf{D})-\text{Arg}(\mathbf{O})$ and $\text{Arg}(\mathbf{O})-\text{Arg}(\mathbf{T})$. Mean values and standard deviations for angular data were calculated by using circular statistics.⁴⁰ Specifically, the angular standard deviation (in radians) was calculated as $\sqrt{2(1-r)}$ where r is the magnitude of the resultant vector of the circular distribution of measured phase angles.⁴¹

By assuming that periodic thigh cuff inflation/deflation does not involve any significant oscillation in the cerebral oxygen consumption (so that its associated phasor can be neglected), the model equations for the phasor ratios $\mathbf{D}(\omega)/\mathbf{O}(\omega)$ and $\mathbf{O}(\omega)/\mathbf{T}(\omega)$ can be written as follows:¹⁸

$$\frac{\mathbf{D}(\omega)}{\mathbf{O}(\omega)} = \frac{(1-S^{(a)})\frac{\Delta\text{CBV}^{(a)}}{\Delta\text{CBV}^{(v)}} + (1-S^{(v)}) - \left[\frac{S^{(c)}}{S^{(v)}} (\langle S^{(c)} \rangle - S^{(v)}) \mathcal{F}^{(c)} \frac{\text{CBV}_0^{(c)}}{\text{CBV}_0^{(v)}} \mathcal{H}_{\text{RC-LP}}^{(c)}(\omega) + (S^{(a)} - S^{(v)}) \mathcal{H}_{G-LP}^{(v)}(\omega) \right] k \frac{\text{CBV}_0^{(c)}}{\text{CBV}_0} \mathcal{H}_{\text{RC-HP}}^{(\text{AutoReg})}(\omega) \left[\frac{\Delta\text{CBV}^{(a)}}{\Delta\text{CBV}^{(v)}} + 1 \right]}{S^{(a)} \frac{\Delta\text{CBV}^{(a)}}{\Delta\text{CBV}^{(v)}} + S^{(v)} + \left[\frac{S^{(c)}}{S^{(v)}} (\langle S^{(c)} \rangle - S^{(v)}) \mathcal{F}^{(c)} \frac{\text{CBV}_0^{(c)}}{\text{CBV}_0^{(v)}} \mathcal{H}_{\text{RC-LP}}^{(c)}(\omega) + (S^{(a)} - S^{(v)}) \mathcal{H}_{G-LP}^{(v)}(\omega) \right] k \frac{\text{CBV}_0^{(v)}}{\text{CBV}_0} \mathcal{H}_{\text{RC-HP}}^{(\text{AutoReg})}(\omega) \left[\frac{\Delta\text{CBV}^{(a)}}{\Delta\text{CBV}^{(v)}} + 1 \right]} \quad (1)$$

$$\frac{\mathbf{O}(\omega)}{\mathbf{T}(\omega)} = \frac{S^{(a)} \frac{\Delta\text{CBV}^{(a)}}{\Delta\text{CBV}^{(v)}} + S^{(v)} + \left[\frac{S^{(c)}}{S^{(v)}} (\langle S^{(c)} \rangle - S^{(v)}) \mathcal{F}^{(c)} \frac{\text{CBV}_0^{(c)}}{\text{CBV}_0^{(v)}} \mathcal{H}_{\text{RC-LP}}^{(c)}(\omega) + (S^{(a)} - S^{(v)}) \mathcal{H}_{G-LP}^{(v)}(\omega) \right] k \frac{\text{CBV}_0^{(v)}}{\text{CBV}_0} \mathcal{H}_{\text{RC-HP}}^{(\text{AutoReg})}(\omega) \left[\frac{\Delta\text{CBV}^{(a)}}{\Delta\text{CBV}^{(v)}} + 1 \right]}{\frac{\Delta\text{CBV}^{(a)}}{\Delta\text{CBV}^{(v)}} + 1} \quad (2)$$

where $\mathcal{F}^{(c)}$ is the Fåhræus factor (i.e., the ratio of capillary to large vessel hematocrit), superscripts (a) , (c) , and (v) for CBV_0 (baseline cerebral blood volume) and S (hemoglobin saturation) indicate partial contributions from the arterial, capillary, and venous compartments; $\mathcal{H}_{\text{RC-LP}}^{(c)}(\omega)$ and $\mathcal{H}_{G-LP}^{(v)}(\omega)$ are the complex transfer functions for the capillary (RC low-pass) and venous (Gaussian time-shifted low-pass) filters respectively;¹⁵ $\Delta\text{CBV}^{(a)}$ and $\Delta\text{CBV}^{(v)}$ represent the amplitude of the oscillations of the arterial and venous blood volume, respectively; k is the inverse of the modified Grubb’s exponent (high-frequency flow-to-volume amplitude ratio), and $\mathcal{H}_{\text{RC-HP}}^{(\text{AutoReg})}(\omega)$ is the RC high-pass transfer function¹⁵ characterized by the cutoff frequency $[(\omega_c^{(\text{AutoReg})})]$ that describes the cerebral autoregulation effects. Autoregulatory effects are modeled by the following expression that describes the dynamic relationship between

the blood flow velocity phasor in the capillary compartment [$\mathbf{cbf}(\omega)$] and blood volume changes [$\mathbf{cbv}(\omega)$].¹⁸

$$\mathbf{cbf}(\omega) = k \mathcal{H}_{\text{RC-HP}}^{(\text{AutoReg})}(\omega) \mathbf{cbv}(\omega) = k \mathcal{H}_{\text{RC-HP}}^{(\text{AutoReg})}(\omega) \times \left[\frac{\text{CBV}_0^{(a)}}{\text{CBV}_0} \mathbf{cbv}^{(a)}(\omega) + \frac{\text{CBV}_0^{(v)}}{\text{CBV}_0} \mathbf{cbv}^{(v)}(\omega) \right]. \quad (3)$$

Here, we set to zero the blood volume changes in the capillary compartment [$\mathbf{cbv}^{(c)}(\omega) = 0$] because of the negligible dynamic dilation and recruitment of capillaries in brain tissue.⁴² We note that the hemoglobin concentration phasors $[\mathbf{O}(\omega)$, $\mathbf{D}(\omega)$, $\mathbf{T}(\omega)]$ have absolute units of micromolar, whereas $\mathbf{cbf}(\omega)$ and $\mathbf{cbv}(\omega)$ are dimensionless since their magnitudes indicate amplitude of oscillations normalized to the baseline (or average) values.^{15,18}

Table 2 Upper and lower limits implemented in the fitting procedure for the six parameters of the hemodynamic model.

	$t^{(c)}$ (s)	$t^{(v)}$ (s)	$\mathcal{F}^{(c)}\text{CBV}_0^{(c)}/\text{CBV}_0^{(v)}$	$\Delta\text{CBV}_0^{(a)}/\Delta\text{CBV}_0^{(v)}$	$\omega_c^{(\text{AutoReg})}/(2\pi)$ (Hz)	$k\text{CBV}_0^{(v)}/\text{CBV}_0$
Lower limit	0.4	1	0.8	0.2	0	0.4
Upper limit	1.4	3	2.4	5	0.15	1.6

Kainerstorfer et al.¹⁸ showed that by taking the ratios $\mathbf{D}(\omega)/\mathbf{O}(\omega)$ and $\mathbf{O}(\omega)/\mathbf{T}(\omega)$ the number of independent parameters in the model is eight, and they can be reduced to six by assuming specific values for α , the rate constant of oxygen diffusion, and $S^{(a)}$, the arterial saturation. Here, we assume the fixed values $\alpha = 0.8 \text{ s}^{-1}$ and $S^{(a)} = 0.98$. Thus, the remaining six unknown parameters of the model are: (1) $t^{(c)}$, (2) $t^{(v)}$, (3) $\mathcal{F}^{(c)}\text{CBV}_0^{(c)}/\text{CBV}_0^{(v)}$, (4) $\Delta\text{CBV}_0^{(a)}/\Delta\text{CBV}_0^{(v)}$, (5) $\omega_c^{(\text{AutoReg})}$, and (6) $k\text{CBV}_0^{(v)}/\text{CBV}_0$.¹⁸ $t^{(c)}$ and $t^{(v)}$ are the mean blood transit times in the capillary and venous compartments, respectively. $\mathcal{F}^{(c)}\text{CBV}_0^{(c)}/\text{CBV}_0^{(v)}$ is the baseline ratio of capillary-to-venous blood volume fraction, and $\Delta\text{CBV}_0^{(a)}/\Delta\text{CBV}_0^{(v)}$ is the amplitude ratio of the arterial-to-venous blood volume oscillations in response to the cyclic thigh cuff inflation. $\omega_c^{(\text{AutoReg})}/(2\pi)$ is the autoregulation cutoff frequency of the high pass filter transfer function [$\mathcal{H}_{\text{RC-HP}}^{(\text{AutoReg})}(\omega)$] that provides a measure of the autoregulation efficiency. Higher cutoff frequencies indicate a broader frequency range in which the brain can efficiently counteract blood pressure changes. Lastly, $k\text{CBV}_0^{(v)}/\text{CBV}_0$ is the venous-to-total blood volume ratio multiplied by the high-frequency flow-to-volume amplitude ratio (k).¹⁸

To identify the best fit between the analytical model expressions of Eqs. (1) and (2) and the four CHS spectra [$|\mathbf{D}|/|\mathbf{O}|$, $|\mathbf{O}|/|\mathbf{T}|$, $\text{Arg}(\mathbf{D})-\text{Arg}(\mathbf{O})$, $\text{Arg}(\mathbf{O})-\text{Arg}(\mathbf{T})$], we used a nonlinear-fitting procedure (function “lsqcurvefit”) available in MATLAB. This algorithm considers the frequency-resolved

measurements of amplitude and phase as input values and, by minimizing a cost function (χ^2) given by the sum of the squares of the fit residuals, finds the best match between data and model by fitting for the six unknown parameters [$t^{(c)}$, $t^{(v)}$, $\mathcal{F}^{(c)}\text{CBV}_0^{(c)}/\text{CBV}_0^{(v)}$, $\Delta\text{CBV}_0^{(a)}/\Delta\text{CBV}_0^{(v)}$, $\omega_c^{(\text{AutoReg})}$, and $k\text{CBV}_0^{(v)}/\text{CBV}_0$] within specific ranges. Following the approach of Kainerstorfer et al.,¹⁸ we have set the upper and lower limits listed in Table 2, which represent physiological ranges for the six parameters.

Fifty-four different initial guesses equally distributed across the considered six-dimensional parameter space (Table 2) were used to explore all associated solutions and their sensitivity to initial guesses. For each initial guess, every single χ^2 value (corresponding to each step of the MATLAB fitting procedure) and the corresponding solution for the six parameters were stored for further analysis. For each subject, only those sets of six parameters corresponding to χ^2 values smaller than a threshold value were selected in order to retain only a subset of best fits. We found that although solutions associated with the smallest χ^2 values generate the best fits, there are other solutions with marginally larger χ^2 values that also result in good fits that lie within one standard deviation of the data for the four measured spectra. The solutions of the six parameters are presented as their respective mean and standard deviation calculated within the χ^2 threshold obtained for each specific subject. Due to the small number of subjects in the two groups, a Wilcoxon rank sum test

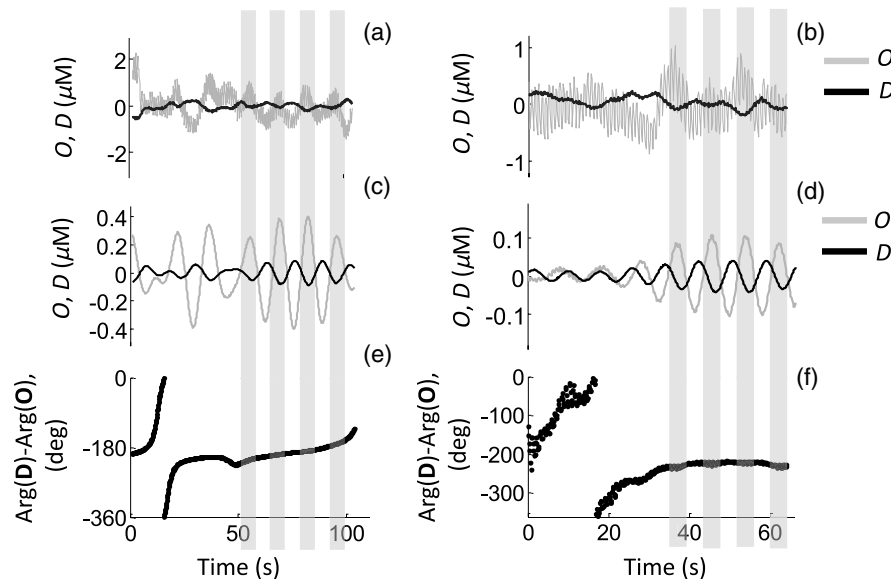


Fig. 2 Representative results recorded on subject 7 during baseline and during four periods of cyclic thigh cuff inflation to a pressure of 200 mmHg (indicated by the shaded areas) at frequencies of 0.07 Hz (left panels) and 0.125 Hz (right panels). (a) and (b) Raw data of deoxy- and oxy-hemoglobin concentrations changes (D and O); (c) and (d) band-pass filtered D and O time traces; (e) and (f) instantaneous phase difference between D and O phasors [$\text{Arg}(\mathbf{D})-\text{Arg}(\mathbf{O})$] at the frequency of cyclic thigh cuff inflation [(e) 0.07 Hz; (f) 0.125 Hz].

was used to test whether there was a statistically significant difference between the average fitting parameters for the hemodialysis patients and the healthy subjects.

3 Results

Figure 2 displays representative time traces of $O(t)$ and $D(t)$ during baseline and cuff occlusions for a healthy subject (Subject 7) at two frequencies of cyclic thigh cuff inflation: 0.07 Hz [panels (a), (c), (e)] and 0.125 Hz [panels (b), (d), (f)]. Unfiltered data [Figs. 2(a)–2(b)] and associated filtered $O(t)$ and $D(t)$ oscillations [Figs. 2(c)–2(d)] are shown for the 0.07- and 0.125-Hz cuff occlusions, respectively. Shaded areas mark the periods of inflated thigh cuff. Panels (e) and (f) show the instantaneous phase difference between $D(t)$ and $O(t)$ before and after cuff occlusion onset for the 0.07- and 0.125-Hz induced oscillations. We observe increased amplitude values for D and O oscillations right after the cuff-occlusion for the 0.125-Hz stimuli [Fig. 2(d)], whereas no significant amplitude increase was observed at 0.07 Hz [Fig. 2(c)]. We also observe greater phase stability for both frequencies during the periodic thigh cuff inflation/deflation with respect to the baseline period [Figs. 2(e) and 2(f)]. These findings, observed in other subjects as well at all frequencies considered, confirm that the periodic thigh cuff occlusion method introduces a good phase stability between the induced O and D oscillations. By contrast, the amplitudes of the induced O and D oscillations consistently exceed the amplitude of baseline spontaneous oscillations only at stimulation frequencies >0.10 Hz.

The measured amplitude and phase spectra for the hemodialysis patients (Subjects 1 to 5) and the healthy subjects (Subjects 6 to 11) are shown in Figs. 3 and 4, respectively. No adjustable scaling factors have been used in the fitting procedures. In both figures, symbols represent the measured data

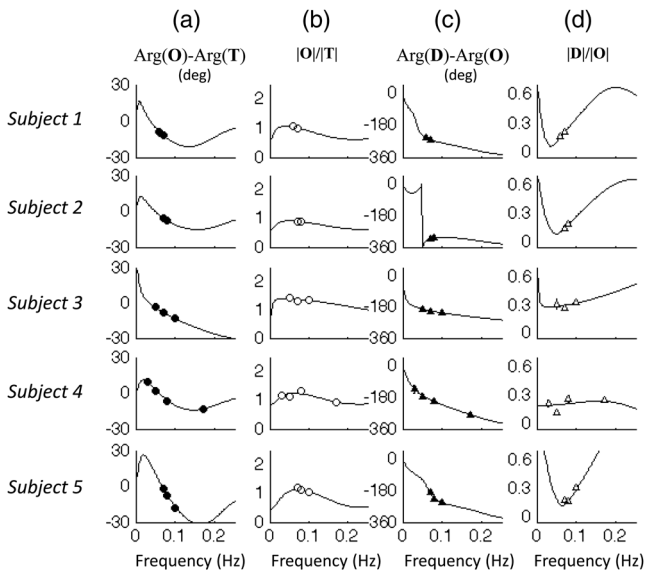


Fig. 3 Coherent hemodynamics spectra (CHS) measured on the forehead of five hemodialysis patients (Subjects 1 to 5) on the basis of measured deoxy-, oxy-, and total hemoglobin concentration phasors $[D(\omega), O(\omega),$ and $T(\omega)]$. (a) Phase difference $\text{Arg}(O)-\text{Arg}(T)$; (b) amplitude ratio $|O|/|T|$; (c) phase difference $\text{Arg}(D)-\text{Arg}(O)$; (d) amplitude ratio $|D|/|O|$. The symbols represent experimental data (error bars are standard deviations), whereas the lines represent the best fits obtained with the hemodynamic model.

whereas lines represent the fits with the smallest χ^2 value obtained with the model Eqs. (1) and (2).

Even though seven different frequencies of cuff inflation were used in all subjects, Figs. 3 and 4 only show the data points that fulfilled our inclusion criteria (presence of a peak in the Fourier spectrum at the stimulation frequency, amplitudes above a set threshold). The data points in the spectra of Figs. 3 and 4 indicate the cases, where it was possible to successfully detect the induced cerebral hemodynamic oscillations with NIRS. We noticed a lower success rate in hemodialysis patients than in healthy subjects. Although healthy subjects measurements were performed in a laboratory environment with highly compliant subjects, hemodialysis patients' measurements were performed in a dialysis unit under more challenging experimental conditions (moving subjects, other clinical/diagnostic devices connected to the patient as part of the hemodialysis procedure, typically larger sense of discomfort experienced by patients during to thigh cuff inflation, etc.).

Our results for the mean and standard deviation of the fitting parameters are shown in Fig. 5. Over the eleven subjects, $t^{(c)}$ ranges from 0.4 to 1.39 s, whereas $t^{(v)}$ ranges from 1.06 to 3.00 s. Figures 5(a) and 5(b) in Fig. 5 show consistently higher capillary and venous blood transit times for the hemodialysis patients with respect to healthy subjects. Differences resulted to be statistically significant ($p < 0.05$, Wilcoxon rank sum test) for both capillary and venous blood transit times. Our measured time constants indicate slower capillary and venous blood flow velocities in hemodialysis patients with respect to healthy subjects.

Panels (c)-(f) of Fig. 5 report the results for the other four fitting parameters, for which we have not observed significant differences between hemodialysis patients and healthy subjects.

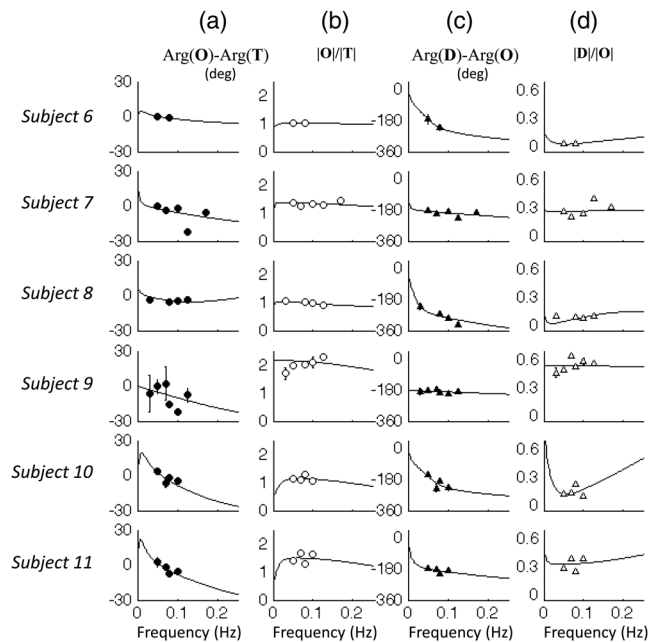


Fig. 4 The CHS measured on the forehead of six healthy subjects (Subjects 6 to 11) on the basis of measured deoxy-, oxy-, and total-hemoglobin concentration phasors $[D(\omega), O(\omega),$ and $T(\omega)]$. (a) Phase difference $\text{Arg}(O)-\text{Arg}(T)$; (b) amplitude ratio $|O|/|T|$; (c) phase difference $\text{Arg}(D)-\text{Arg}(O)$; (d) amplitude ratio $|D|/|O|$. The symbols represent experimental data (error bars are standard deviations when larger than the symbol size), whereas the lines represent the best fits obtained with the hemodynamic model.

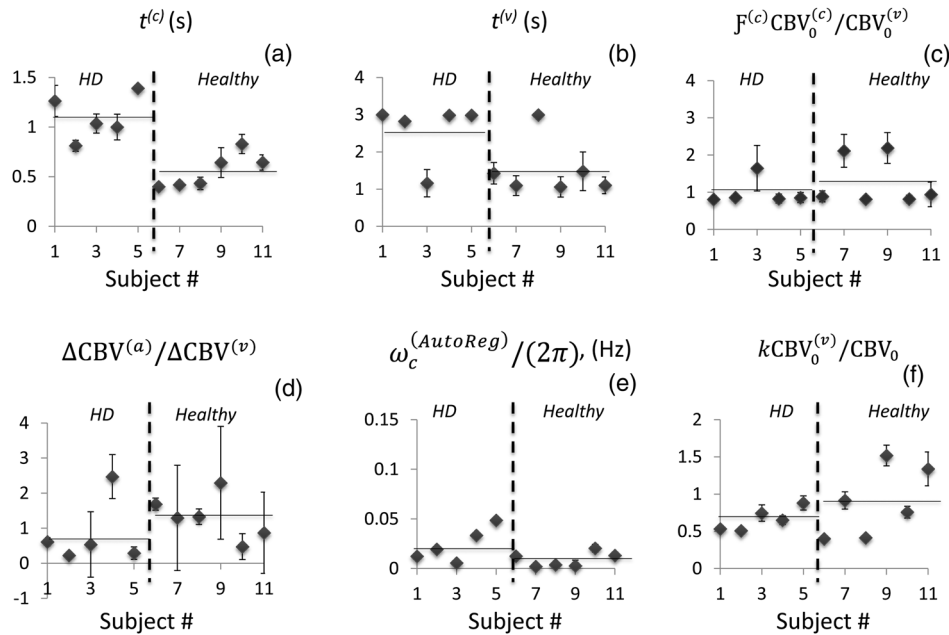


Fig. 5 Summary of our results for the six fitting parameters, expressed as mean \pm standard deviation, for the five hemodialysis patients (HD) (subjects 1 to 5) and the six healthy subjects (subjects 6 to 11). Horizontal lines are the average values for each of the six parameters for the two groups. (a) blood transit time in the capillary compartment [$t^{(c)}$]; (b) blood transit time in the venous compartment [$t^{(v)}$]; (c) baseline capillary-to-venous blood volume ratio [$F^{(c)}CBV_0^{(c)}/CBV_0^{(v)}$]; (d) ratio of the arterial-to-venous amplitude of blood volume oscillations [$\Delta CBV_0^{(a)}/\Delta CBV_0^{(v)}$]; (e) autoregulation cutoff frequency [$\omega_c^{(AutoReg)}/(2\pi)$]; (f) high-frequency flow-to-volume amplitude ratio times the venous-to-total blood volume ratio [$kCBV_0^{(v)}/CBV_0$].

In particular, we have found no significant difference between the cut-off frequencies for autoregulation in the two groups. Our measured autoregulation cutoff frequency [$\omega_c^{(AutoReg)}/(2\pi)$] values range between 0.02 and 0.05 Hz in all measured subjects. These values are lower than the autoregulation cut-off frequency reported on the basis of arterial blood pressure and flow velocity measurements (0.15 Hz).⁴³ This difference may reflect the fact that NIRS measurements and CHS assess local microcirculation phenomena, whereas finger plethysmography and transcranial Doppler ultrasound assess systemic and macrocirculation effects.

We conclude this section by observing that in the cases in which the fitting parameters took values at the set limits of Table 2, we found that the quality of the fits would not significantly improve by letting the fitting parameters take values outside of the physiological ranges of Table 2.

4 Discussion

We have reported a new set of frequency-resolved measurements of cerebral hemodynamic oscillations measured with NIRS in hemodialysis patients and healthy controls. We have induced hemodynamic oscillations at controlled frequencies by cyclic thigh cuff occlusions, and analyzed the NIRS data according to the recently proposed technique of CHS.¹⁵ Among a number of possible protocols to induce hemodynamic oscillations, we have used a passive protocol (cuff occlusion of the thigh) for its applicability in a clinical environment and for its high level of automation and reproducibility. The minimum amount of time required to measure our CHS, based on seven different stimulation frequencies (0.03 to 0.17 Hz), was ~ 14 min plus several minutes to position the thigh cuff and the NIRS probe on the subjects' forehead. Because of patients' time constraints before dialysis onset and after treatment, the CHS

measurements were only performed during the dialysis procedure itself. Although cuff occlusions were performed at seven frequencies between 0.03 and 0.17 Hz, the measured CHS spectra indicate the range 0.05 to 0.10 Hz as the most successful frequencies to induce measurable periodic oscillations in the cerebral hemodynamics. The acquisition time for CHS may be shortened by performing online detection of reliably induced hemodynamic oscillations. Furthermore, rest periods between stimuli at different frequencies may be shortened or eliminated, and multiple frequencies may be excited simultaneously by introducing specially shaped temporal stimulations (step function, cycles with variable periods, etc.). Another approach to speeding up the collection of the CHS data is to consider one single period for each frequency of induced oscillations. Each stimulus in this study consisted of four inflation/deflation periods. In principle, a single $D(t)$ and $O(t)$ period is sufficient to assess the amplitude ratios and phase differences necessary to CHS analysis as we have previously observed in a study based on a paced breathing protocol.¹⁶ However, in this work, we found that multiple inflation/deflation periods may be required to achieve a stable phase relationship between cerebral D and O oscillations, and this may depend on the specific protocol/application considered.

We observed increased amplitudes of D and O oscillations in response to the periodic thigh cuff inflation for frequencies above 0.1 Hz (see Fig. 2). At lower frequencies, the presence of strong spontaneous LFOs^{6,44} may explain the lack of enhanced oscillations at the thigh cuff inflation frequency. However, despite a lack of enhanced amplitude, even at frequencies below 0.1 Hz we have found an improved phase stability of the induced oscillations, indicating some level of synchronization of intrinsic cerebral hemodynamic oscillations at the frequency of the thigh cuff inflation.

Measured CHS spectra, combined with Fantini's hemodynamic model,¹⁶ allowed for the measurement of several physiological parameters. The major results of this study are the longer blood transit times [$t^{(c)}$ and $t^{(v)}$] in hemodialysis patients with respect to healthy subjects. Longer capillary and venous blood transit times correspond to a reduced cerebral blood flow velocity in the microcirculation. Reduced blood flow velocity in the middle cerebral artery has been repeatedly measured by transcranial Doppler ultrasound during hemodialysis,^{24,26,32,45,46} and it has been tentatively associated with increased blood viscosity^{26,33} or oxygen carrying capacity alterations.^{26,33} Our findings on the hemodialysis patients, all measured within the first hour of the hemodialysis procedure, indicate a reduced blood flow velocity with respect to the healthy control group, suggesting either a chronically reduced flow velocity for this population, or a relatively rapid decrease in flow velocity that is associated with the initiation of the hemodialysis procedure. These results are consistent with transcranial Doppler findings²³ conducted pre and posthemodialysis, which showed a significant lower flow velocity values for patients at the start of hemodialysis with respect to healthy controls. We observe, however, that our study did not feature age-matched clinical and control groups, so that aging effects may have contributed to our results. More studies are required to investigate the specific clinical conditions and aging effects contributions to the observed reduction in microvascular cerebral blood flow.

Our results for the autoregulation cut-off frequency [$\omega_c^{(\text{AutoReg})}/(2\pi)$] do not indicate a significant difference between the autoregulation efficiency in hemodialysis patients ($n = 5$) and healthy subjects ($n = 6$). It has been found that specific cohorts of hemodialysis patients feature normal autoregulation,³² and that the hemodialysis procedure does not directly impact cerebral autoregulation,^{32,46} even though one case study reported that intermittent hemodialysis could negatively impact autoregulation.⁴⁷ However, some critically ill hemodialysis patients did feature a significantly impaired autoregulation,⁴⁸ and some comorbid conditions such as vascular disease and old age may account for impaired autoregulation in hemodialysis patients.⁴⁹ Of note, all hemodialysis sessions reported here were clinically uneventful, with heart rate and mean arterial pressures before and after dialysis remaining stable.

5 Conclusions

We have presented the first clinical demonstration of CHS¹⁵ by performing frequency-resolved NIRS measurements of cerebral hemodynamic oscillations induced by cyclic thigh cuff occlusions in hemodialysis patients and healthy subjects. Measured CHS spectra, combined with the quantitative analysis carried out with Fantini's model,^{15,50} allowed for the assessment of several physiological parameters in a clinical setting, namely the dialysis unit, therefore showing potential for clinical as well as research studies. Because of the critical importance of cerebral hemodynamics at the microcirculation level, the proposed method lends itself to a broad range of applications, including functional brain studies, anesthesia, stroke, traumatic brain injury, neurovascular disorders, etc. Future research should identify optimal protocols for investigating cerebral hemodynamic oscillations (either spontaneous or induced) over a range of frequencies, methods to reduce the time required for the collection of CHS spectra, efficient fitting procedures to obtain reliable measures of the accessible physiological parameters, and extension of the CHS method to spatially resolved

approaches for either mapping or depth-resolved measurements. These prospects may open new opportunities for research and clinical applications, and may lead to a new class of tools to study the cerebral hemodynamics with near infrared spectroscopy.

Acknowledgments

This research is supported by the National Institutes of Health (Grant no. R01-CA154774) and by the National Science Foundation (Award no. IIS-1065154).

References

1. T. Katura et al., "Quantitative evaluation of interrelations between spontaneous low-frequency oscillations in cerebral hemodynamics and systemic cardiovascular dynamics," *NeuroImage* **31**(4), 1592–1600 (2006).
2. M. D. Fox and M. E. Raichle, "Spontaneous fluctuations in brain activity observed with functional magnetic resonance imaging," *Nat. Rev. Neurosci.* **8**(9), 700–711 (2007).
3. B. R. White et al., "Resting-state functional connectivity in the human brain revealed with diffuse optical tomography," *NeuroImage* **47**(1), 148–156 (2009).
4. H. Obrig et al., "Spontaneous low frequency oscillations of cerebral hemodynamics and metabolism in human adults," *NeuroImage* **12**(6), 623–639 (2000).
5. A. Sassaroli et al., "Phase difference between low-frequency oscillations of cerebral deoxy- and oxy-hemoglobin concentrations during a mental task," *J. Innov. Opt. Health. Sci.* **4**(2), 151–158 (2011).
6. M. L. Pierro et al., "Phase-amplitude investigation of spontaneous low-frequency oscillations of cerebral hemodynamics with near-infrared spectroscopy: a sleep study in human subjects," *NeuroImage* **63**(3), 1571–1584 (2012).
7. R. R. Diehl et al., "Spontaneous blood pressure oscillations and cerebral autoregulation," *Clin. Auton. Res.* **8**(1), 7–12 (1998).
8. M. Reinhard et al., "Transfer function analysis for clinical evaluation of dynamic cerebral autoregulation—a comparison between spontaneous and respiratory-induced oscillations," *Physiol. Meas.* **24**(1), 27–43 (2003).
9. P. J. Eames, J. F. Potter, and R. B. Panerai, "Influence of controlled breathing patterns on cerebrovascular autoregulation and cardiac baroreceptor sensitivity," *Clin. Sci. (Lond)* **106**(2), 155–162 (2004).
10. R. L. Hughson et al., "Critical analysis of cerebrovascular autoregulation during repeated head-up tilt," *Stroke* **32**(10), 2403–2408 (2001).
11. J. A. Claassen, B. D. Levine, and R. Zhang, "Dynamic cerebral autoregulation during repeated squat-stand maneuvers," *J. Appl. Physiol.* **106**(1), 153–160 (2009).
12. R. Aaslid et al., "Asymmetric dynamic cerebral autoregulatory response to cyclic stimuli," *Stroke* **38**(5), 1465–1469 (2007).
13. J. Frederiks et al., "The importance of high-frequency paced breathing in spectral baroreflex sensitivity assessment," *J. Hypertens.* **18**(11), 1635–1644 (2000).
14. M. A. Franceschini et al., "Diffuse optical imaging of the whole head," *J. Biomed. Opt.* **11**(5), 054007 (2006).
15. S. Fantini, "Dynamic model for the tissue concentration and oxygen saturation of hemoglobin in relation to blood volume, flow velocity, and oxygen consumption: implications for functional neuroimaging and coherent hemodynamics spectroscopy," *NeuroImage* **85**, 202–221 (2014).
16. M. L. Pierro et al., "Validation of a novel hemodynamic model for coherent hemodynamics spectroscopy (CHS) and functional brain studies with fNIRS and fMRI," *NeuroImage* **85**, 222–233 (2014).
17. J. M. Kainerstorfer et al., "Coherent Hemodynamics Spectroscopy based on a paced breathing paradigm-revisited," *J. Innov. Opt. Health. Sci.* **7**(1), 1450013 (2014).
18. J. M. Kainerstorfer et al., "Practical steps for applying a new dynamic model to near-infrared spectroscopy measurements of hemodynamic oscillations and transient changes," *Acad. Radiol.* **21**(2), 185–196 (2014).

19. M. J. Sarnak and A. S. Levey, "Cardiovascular disease and chronic renal disease: a new paradigm," *Am. J. Kidney Dis.* **35**(4 Suppl 1), S117–S131 (2000).
20. D. E. Weiner et al., "Cardiovascular outcomes and all-cause mortality: exploring the interaction between CKD and cardiovascular disease," *Am. J. Kidney Dis.* **48**(3), 392–401 (2006).
21. S. L. Seliger et al., "Cystatin C and subclinical brain infarction," *J. Am. Soc. Nephrol.* **16**(12), 3721–3727 (2005).
22. D. A. Drew et al., "Anatomic brain disease in hemodialysis patients: a cross-sectional study," *Am. J. Kidney Dis.* **61**(2), 271–278 (2013).
23. I. Prohovnik et al., "Cerebrovascular effects of hemodialysis in chronic kidney disease," *J. Cereb. Blood Flow Metab.* **27**(11), 1861–1869 (2007).
24. G. Papadopoulos et al., "Cerebral oximetry values in dialyzed surgical patients: a comparison between hemodialysis and peritoneal dialysis," *Ren. Fail.* **35**(6), 855–859 (2013).
25. R. A. De Blasi et al., "Microcirculatory changes and skeletal muscle oxygenation measured at rest by non-infrared spectroscopy in patients with and without diabetes undergoing haemodialysis," *Crit. Care* **13**(9), S9 (2009).
26. D. Gottlieb et al., "The regional cerebral blood flow in patients under chronic hemodialytic treatment," *J. Cereb. Blood Flow Metab.* **7**(5), 659–661 (1987).
27. J. Kwiecinski et al., "Influence of hemodialysis on changes in cerebral artery blood flow velocity in patients with chronic renal failure," *Pol. Arch. Med. Wewn.* **96**(1), 8–14 (1996).
28. G. Regolisti et al., "Cerebral blood flow decreases during intermittent hemodialysis in patients with acute kidney injury, but not in patients with end-stage renal disease," *Nephrol. Dial. Transplant.* **28**(1), 79–85 (2013).
29. I. Stefanidis et al., "Influence of hemodialysis on the mean blood flow velocity in the middle cerebral artery," *Clin. Nephrol.* **64**(2), 129–137 (2005).
30. A. Postiglione et al., "Changes in middle cerebral artery blood velocity in uremic patients after hemodialysis," *Stroke* **22**(12), 1508–1511 (1991).
31. I. Prohovnik et al., "Cerebrovascular effects of hemodialysis in chronic kidney disease," *J. Cereb. Blood Flow Metab.* **27**(11), 1861–1869 (2007).
32. H. Skinner et al., "Cerebral haemodynamics in patients with chronic renal failure: effects of haemodialysis," *Br. J. Anaesth.* **94**(2), 203–205 (2005).
33. R. Hata et al., "Effects of hemodialysis on cerebral circulation evaluated by transcranial Doppler ultrasonography," *Stroke* **25**(2), 408–412 (1994).
34. A. Sassaroli and S. Fantini, "Comment on the modified Beer-Lambert law for scattering media," *Phys. Med. Biol.* **49**(14), N255-7 (2004).
35. S. Fantini et al., "Non-invasive optical monitoring of the newborn piglet brain using continuous-wave and frequency-domain spectroscopy," *Phys. Med. Biol.* **44**(6), 1543–1563 (1999).
36. T. Parks and J. McClellan, "Chebyshev approximation for nonrecursive digital filters with linear phase," *IEEE Trans. Circuit Theory* **19**(2), 189–194 (1972).
37. M. L. Pierro et al., "Relative phase of oscillations of cerebral oxy-hemoglobin and deoxy-hemoglobin concentrations during sleep," *Proc. SPIE* **8207**, 82074Y (2012).
38. D. Gabor, "Theory of communication," *J. Inst. Elect. Eng. (London)* **93**, 429–457 (1946).
39. P. Tass et al., "Detection of n:m phase locking from noisy data: application to magnetoencephalography," *Phys. Rev. Lett.* **81**, 3291–3294 (1998).
40. P. Berens, "A MATLAB toolbox for circular statistics," *J. Stat. Software* **31**(10), 1–21 (2009).
41. J. H. Zar, *Biostatistical Analysis*, 5th ed., Prentice Hall, Upper Saddle River, New Jersey (2010).
42. U. Gobel et al., "Lack of capillary recruitment in the brains of awake rats during hypercapnia," *J. Cereb. Blood Flow Metab.* **9**(4), 491–499 (1989).
43. A. P. Blaber et al., "Transfer function analysis of cerebral autoregulation dynamics in autonomic failure patients," *Stroke* **28**(9), 1686–1692 (1997).
44. F. Tian et al., "Enhanced functional brain imaging by using adaptive filtering and a depth compensation algorithm in diffuse optical tomography," *IEEE Trans. Med. Imaging* **30**(6), 1239–1251 (2011).
45. H. Holzer et al., "The effects of haemodialysis on cerebral blood flow," *Proc. Eur. Dial. Transplant Assoc.* **18**, 126–132 (1981).
46. G. Metry et al., "Online monitoring of cerebral hemodynamics during hemodialysis," *Am. J. Kidney Dis.* **40**(5), 996–1004 (2002).
47. S. B. Ko et al., "Pearls & Oysters: the effects of renal replacement therapy on cerebral autoregulation," *Neurology* **78**(6), e36–e38 (2012).
48. P. Schramm et al., "Cerebrovascular autoregulation in critically ill patients during continuous hemodialysis," *Can. J. Anaesth.* **60**(6), 564–569 (2013).
49. M. Madero and M. J. Sarnak, "Does hemodialysis hurt the brain?" *Semin. Dial.* **24**(3), 266–268 (2011).
50. S. Fantini, "A new hemodynamic model shows that temporal perturbations of cerebral blood flow and metabolic rate of oxygen cannot be measured individually using functional near-infrared spectroscopy," *Physiol. Meas.* **35**(1), N1–N9 (2014).

Biographies of the authors are not available.